

# Electronic Supplementary Information

## Regioisomer-Manipulating Thio-Perylenediimide Nanoagents for Photothermal/Photodynamic Theranostics

*Zhonghua Liu,<sup>a</sup> Yijian Gao,<sup>a</sup> Xin Jin,<sup>b</sup> Qingyuan Deng,<sup>a</sup> Zengle Yin,<sup>a</sup> Shuaihang Tong,<sup>b</sup> Weixia Qing<sup>a\*</sup> and Yongwei Huang<sup>a\*</sup>*

<sup>a</sup>Laboratory for NanoMedical Photonics, School of Basic Medical Science, Henan University, Kaifeng 475004, China.

E-mail: qingwx@henu.edu.cn (W. Qing) and hywei79@126.com (Y. Huang)

<sup>b</sup>School of Pharmacy, Henan University, Kaifeng 475004, China.

Table S1. Photophysical properties of reported perylene agents.

PTT agents	PCE (%)	Laser irradiation	Concentration
<b>PLAC-PDI NPs</b> <sup>1</sup>	42%	730 nm, 0.5 W cm <sup>-2</sup>	0.60 mg mL <sup>-1</sup>
<b>TNMs</b> <sup>2</sup>	41 %	660 nm, 1 W cm <sup>-2</sup>	50 μM
<b>PDS-PDI</b> <sup>3</sup>	40 %	660 nm, 0.5 W cm <sup>-2</sup>	0.5 mg mL <sup>-1</sup>
<b>PDI-PEG</b> <sup>4</sup>	43%	660 nm, 1W cm <sup>-2</sup>	100 μg mL <sup>-1</sup>

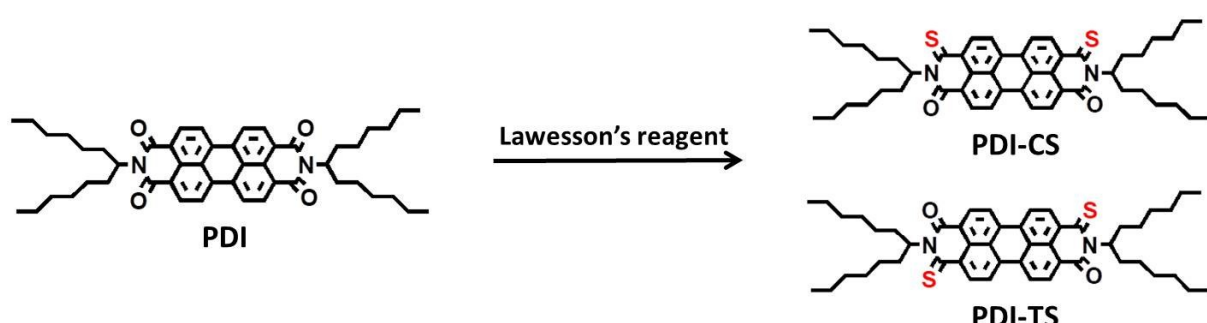


Fig. S1. Synthesis and structures of PDI-CS and PDI-TS.

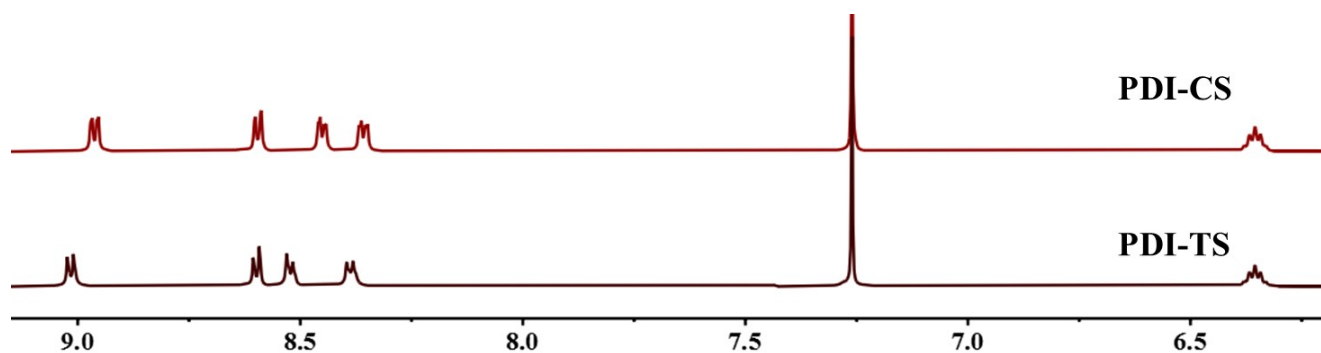


Fig. S2. Partial <sup>1</sup>H NMR spectra of PDI-CS, PDI-TS.

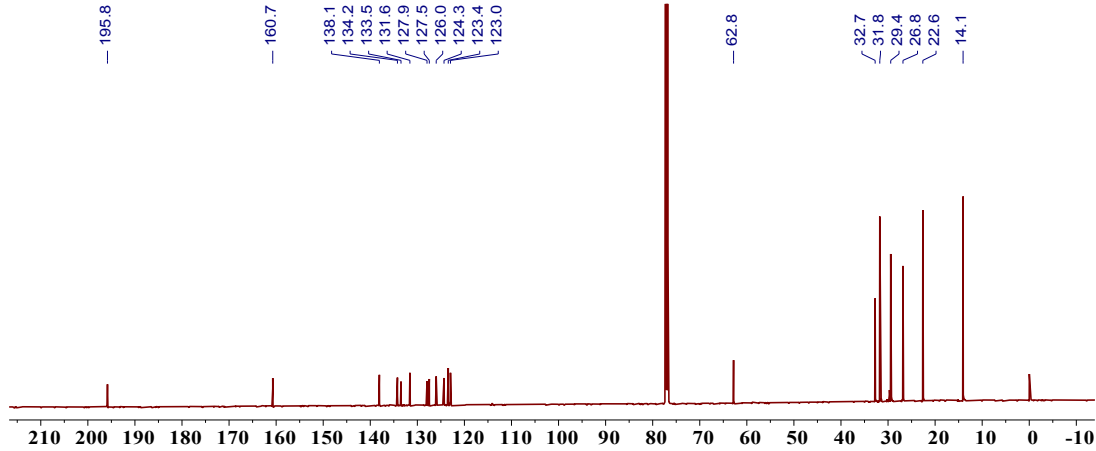


Fig. S3.  $^{13}\text{C}$  NMR spectrum of PDI-CS.

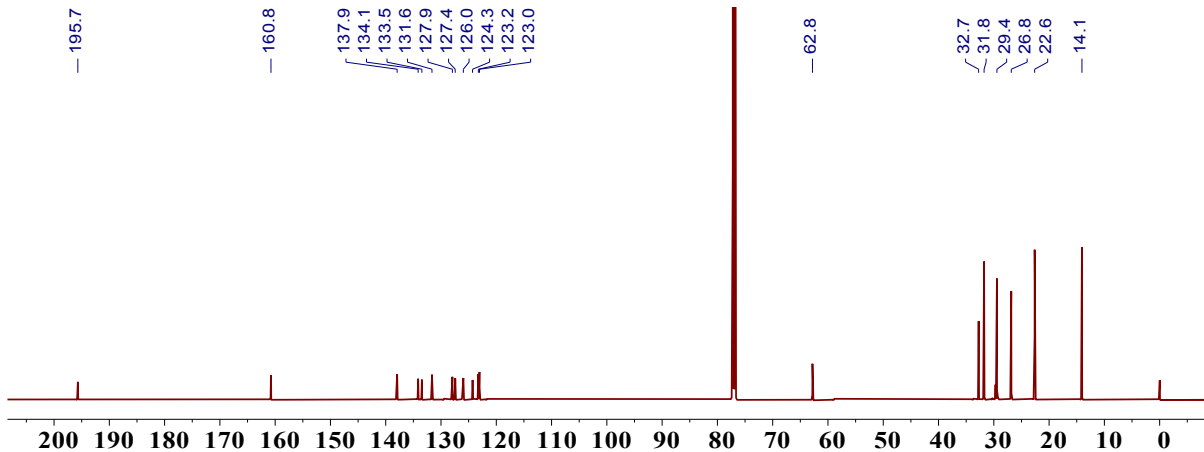


Fig. S4.  $^{13}\text{C}$  NMR spectrum of PDI-TS.

National Center for Organic Mass Spectrometry in Shanghai  
Shanghai Institute of Organic Chemistry  
Chinese Academic of Sciences  
High Resolution MS DATA REPORT



Instrument: Thermo Fisher Scientific LTQ FT Ultra

Card Serial Number : D20200628

Sample Serial Number: PDI-CS

Operator : DONG Date: 2020/04/03

Operation Mode: DART POSITIVE

#### Elemental composition search on mass 787.43

m/z	Theo. Mass	Delta (ppm)	RDB equiv	Composition
787.4323	787.4325	-0.34	20.5	C <sub>50</sub> H <sub>63</sub> O <sub>2</sub> N <sub>2</sub> S <sub>2</sub>
	787.4332	-1.17	29.5	C <sub>58</sub> H <sub>59</sub> S
	787.4312	1.37	21.0	C <sub>48</sub> H <sub>61</sub> ON <sub>5</sub> S <sub>2</sub>
	787.4344	-2.64	26.0	C <sub>52</sub> H <sub>57</sub> O <sub>4</sub> N <sub>3</sub>
	787.4299	3.06	16.0	C <sub>47</sub> H <sub>65</sub> O <sub>5</sub> N <sub>2</sub> S
	787.4292	3.94	25.5	C <sub>53</sub> H <sub>59</sub> O <sub>2</sub> N <sub>2</sub> S
	787.4357	-4.34	25.5	C <sub>54</sub> H <sub>59</sub> O <sub>5</sub>
	787.4285	4.77	16.5	C <sub>45</sub> H <sub>63</sub> O <sub>4</sub> N <sub>4</sub> S <sub>2</sub>

Fig.S5. HRMS of PDI-CS. calcd for C<sub>50</sub>H<sub>62</sub>N<sub>2</sub>O<sub>2</sub>S<sub>2</sub>, 786.4253 m/z, found [M+H]<sup>+</sup> 787.4323.



Instrument: Thermo Fisher Scientific LTQ FT Ultra

Card Serial Number : D20200630

Sample Serial Number: PDI-TS

Operator : DONG Date: 2020/04/03

Operation Mode: DART POSITIVE

Elemental composition search on mass 787.43

m/z	Theo. Mass	Delta (ppm)	RDB equiv.	Composition
787.4323	787.4325	-0.35	20.5	C <sub>50</sub> H <sub>63</sub> O <sub>2</sub> N <sub>2</sub> S <sub>2</sub>
	787.4332	-1.18	29.5	C <sub>50</sub> H <sub>65</sub> S
	787.4312	1.35	21.0	C <sub>48</sub> H <sub>61</sub> ON <sub>5</sub> S <sub>2</sub>
	787.4344	-2.65	26.0	C <sub>52</sub> H <sub>57</sub> O <sub>4</sub> N <sub>3</sub>
	787.4299	3.05	16.0	C <sub>47</sub> H <sub>65</sub> OS <sub>2</sub>
	787.4292	3.93	25.5	C <sub>53</sub> H <sub>65</sub> O <sub>2</sub> N <sub>2</sub> S
	787.4357	-4.36	25.5	C <sub>54</sub> H <sub>65</sub> O <sub>5</sub>
	787.4285	4.76	16.5	C <sub>45</sub> H <sub>63</sub> O <sub>4</sub> N <sub>4</sub> S <sub>2</sub>

Fig. S6. HRMS of PDI-TS. calcd for C<sub>50</sub>H<sub>62</sub>N<sub>2</sub>O<sub>2</sub>S<sub>2</sub>, 786.4253 m/z, found [M+H]<sup>+</sup> 787.4323.

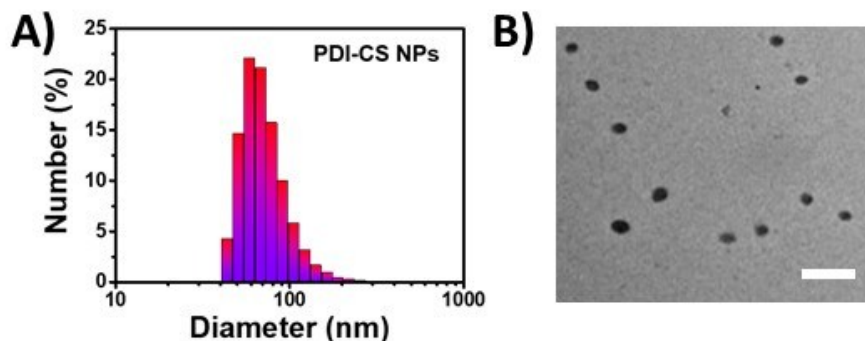


Fig. S7. (A) DLS measurement and (B) TEM image PDI-CS NPs (scale bar: 200 nm).

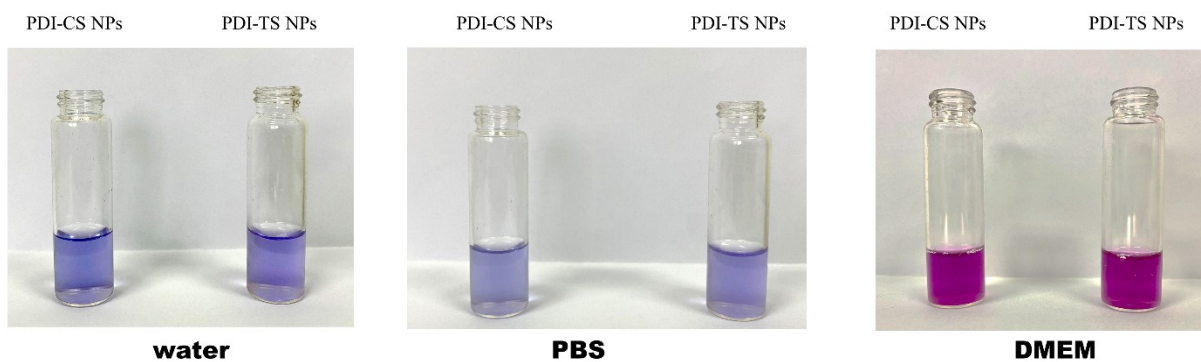


Fig. S8. The stability of PDI-CS and PDI-TS NPs in different solution after being stored in 4 °C refrigerator for four weeks.

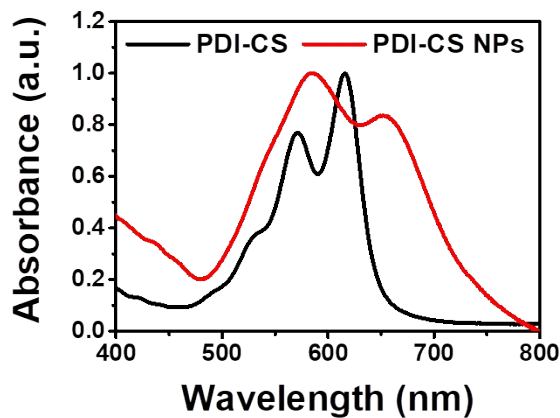


Fig. S9. UV-vis absorption spectra of PDI-CS in THF and NPs in deionized water.

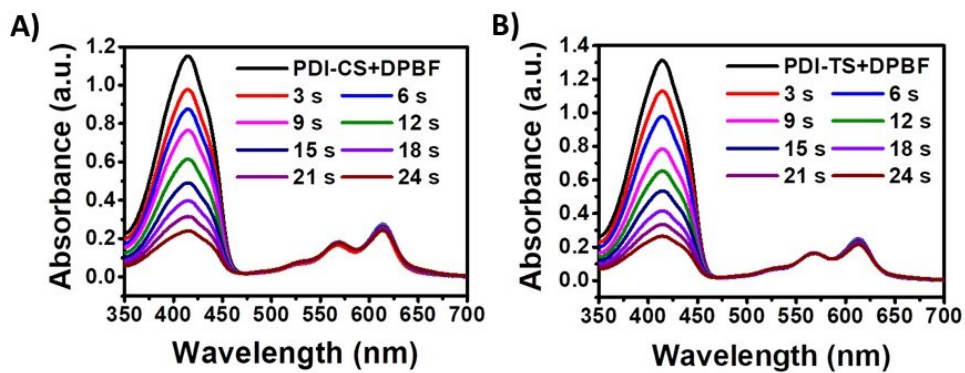


Fig. S10. Absorbance of (A) PDI-CS and (B) PDI-TS with DPBF after photodecomposition by ROS generation upon light irradiation at  $20 \text{ mW cm}^{-2}$ .

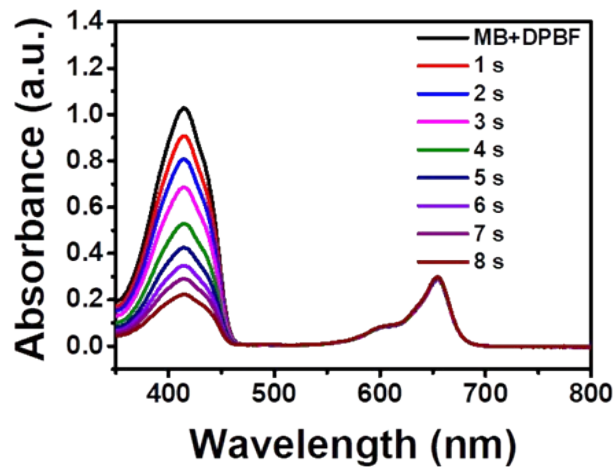


Fig. S11. Absorbance of DPBF after methylene blue (MB) by ROS generation upon light irradiation at  $20 \text{ mW cm}^{-2}$ .

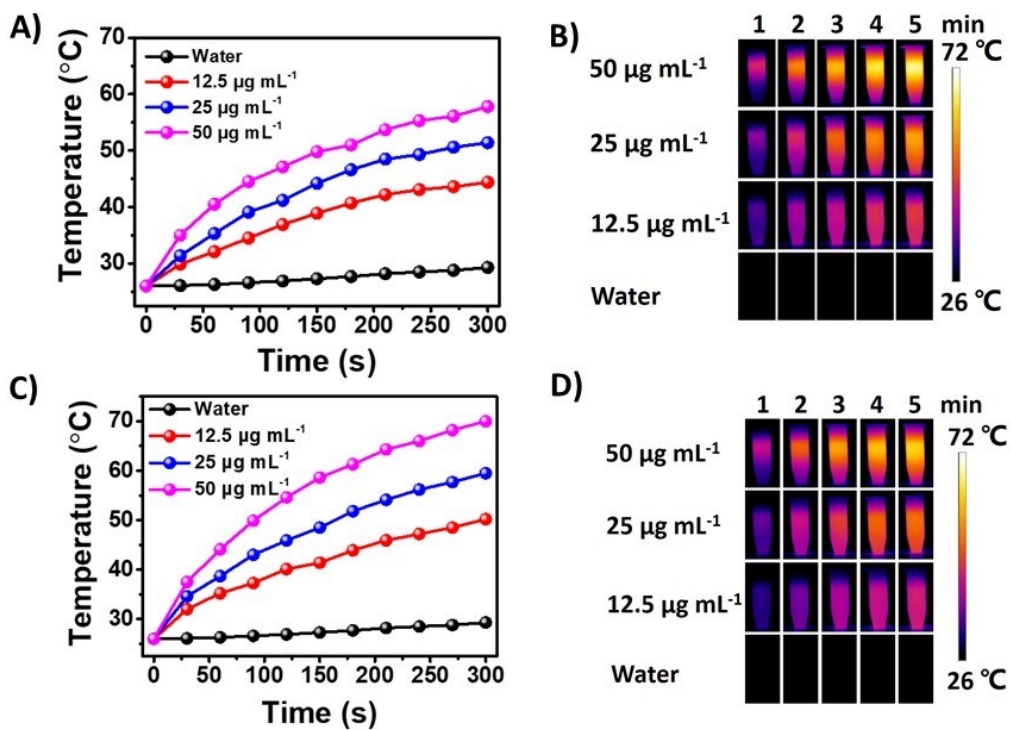


Fig. S12. (A, C) Temperature elevation and (B, D) infrared thermographs of (A, B) PDI-CS and (C, D) PDI-TS NPs aqueous solutions under 660 nm irradiation for 5 min ( $0.75 \text{ W cm}^{-2}$ ).

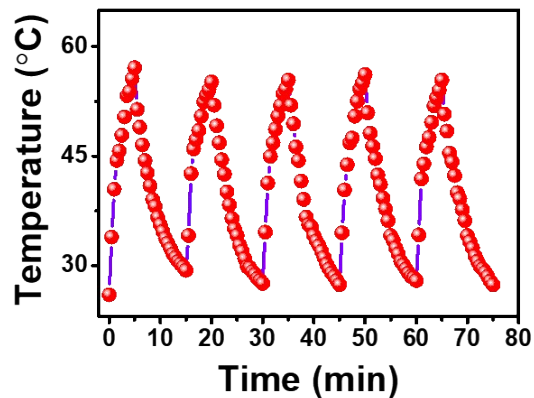


Fig. S13. Temperature profiles of a PDI-CS NPs aqueous dispersion for five laser on/off cycles.

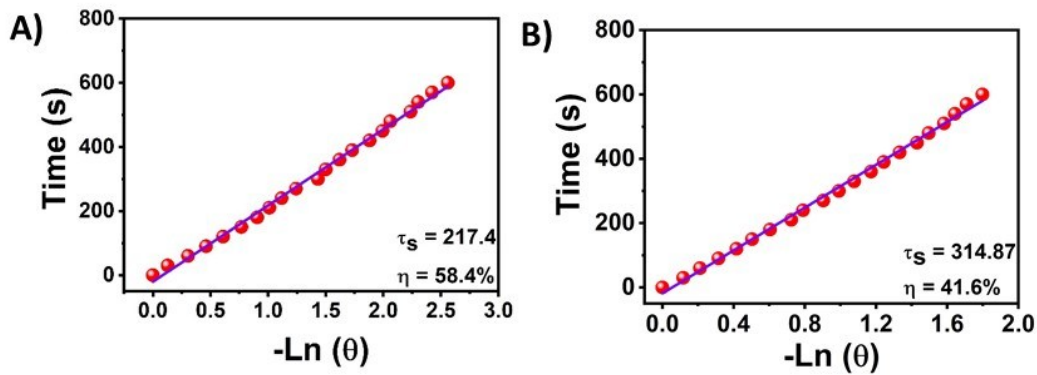


Fig. S14. A plot of time against temperature during the cooling period of (A) PDI-TS NPs and (B) PDI-CS NPs aqueous solution ( $50 \mu\text{g mL}^{-1}$ ) under irradiation for 10 min with a laser (660 nm,  $0.75 \text{ W cm}^{-2}$ ).

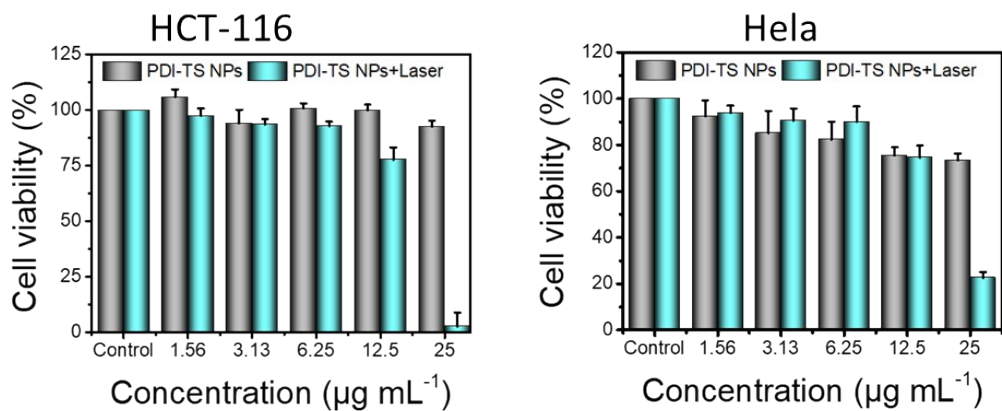


Fig. S15. Cell viability of HCT-116 and HeLa cells after treatment with PDI-TS at different concentrations (0, 1.56, 3.13, 6.25, 12.5, 25  $\mu\text{g mL}^{-1}$ ) plus with 660 nm laser irradiation at  $0.75 \text{ W cm}^2$  for 5 min.

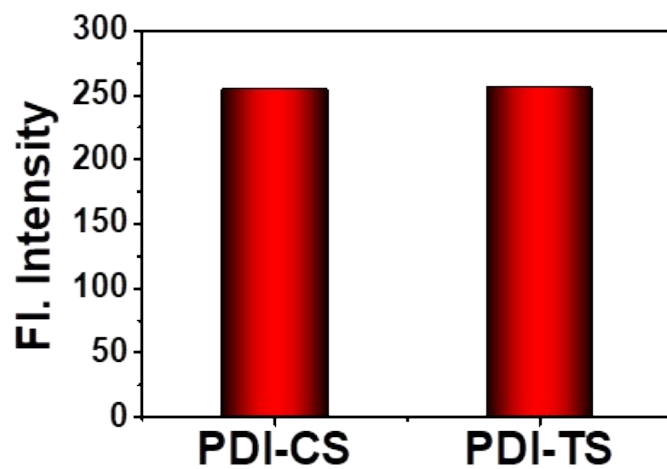


Fig. S16. Fluorescence intensity analysis of ROS production.

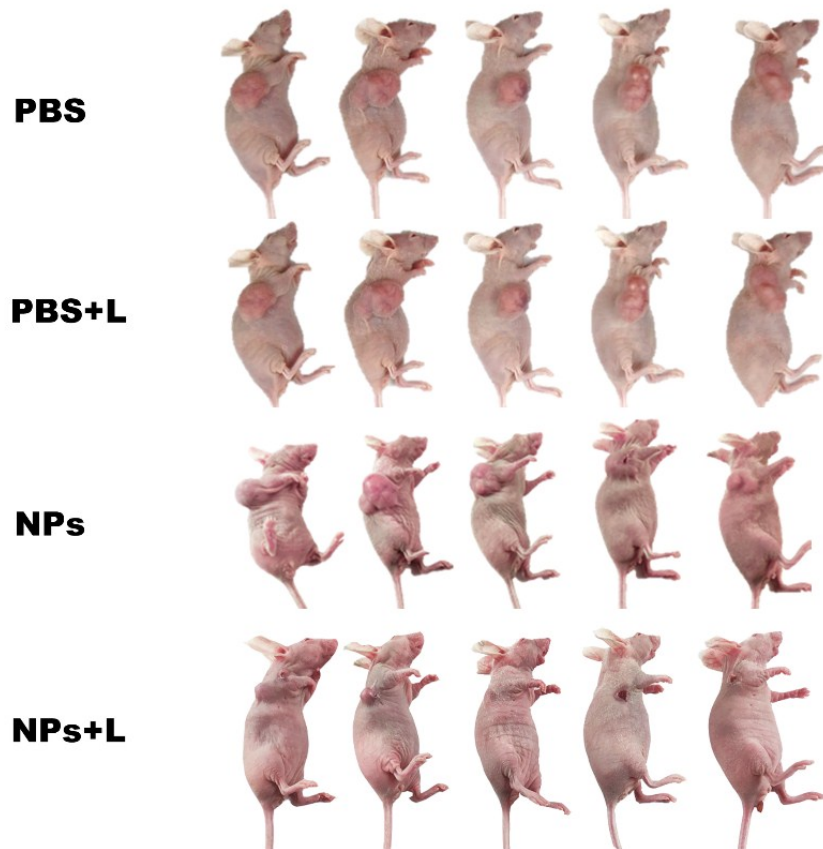


Fig. S17. Representative pictures of tumor-bearing mice after different treatments.

## References

- 1 P. Sun, P. Yuan, G. Wang, W. Deng, S. Tian, C. Wang, X. Lu, W. Huang and Q. Fan, *Biomacromolecules* 2017, **18**, 3375.
- 2 S. Zhang, W. Guo, J. Wei, C. Li , X. Liang and M. Yin, *ACS Nano* 2017, **11**, 3797.
- 3 P. Sun , X. Wang , G. Wang, W. Deng, Q. Shen, R. Jiang, W. Wang, Q. Fan and W. Huang, *J. Mater. Chem. B*. 2018, **6**, 3395
- 4 S. Zhang, J. Li, J. Wei and M. Yin, *Sci. Bull.* 2018, **63**, 101.